Volume 15, Issue 3, 152419 (1-15)

International Journal of Nano Dimension (IJND)

https://dx.doi.org/10.57647/j.ijnd.2024.1503.19

Evaluation of phytochemicals, anti-oxidative properties and synergistic effects of green fabricated AuNPs-GrNs nanocomposites against selected Gram-positive and Gram-negative bacterial strains

Sarita Yadav, Neetu Sehrawat, Minakshi Sharma*

Department of Zoology, Maharshi Dayanand University, Haryana, India.

***Corresponding author:** sminakshi.2007@rediffmail.com

Original Research

Received:
24 January 2024
Revised:
17 March 2024
Accepted:
28 March 2024
Published online:
15 June 2024

Abstract:

Graphene and its derivatives are biocompatible, have a huge surface area, good resistance capacity and thermal conductivity. The unique features listed above are extremely important for killing microorganisms. This paper presents the fabrication of gold nanoparticles (AuNPs), graphene nanosheets (GrNs), and GrNs functionalized with AuNPs by a novel eco-friendly method. These GrNs and AuNPs were fabricated by using leaf extracts of *Syzygium cumini* and *Passiflora edulis* respectively, as novel reducing agents. AuNPs were successfully embedded on fabricated GrNs. Embedded AuNPs increased the surface area, sensitivity, and conductivity of GrNs and acted as nano-spacers between sheets. Energy dispersive X-ray showed the Au, C, and O elemental composition in AuNPs-GrNs nanocomposite that confirmed the formation of the nanocomposite. A comparative antibacterial activity of AuNPs, GrNs, and AuNPs-GrNs nanocomposite was studied against Gram +ve (*Bacillus subtilis, Staphylococcus aureus*), and Gram -ve (*Escherichia coli, Pseudomonas aeruginosa*) bacterial strains.

Keywords: Antioxidative property; Bactericidal effects; Graphene nanosheets; Gold nanoparticles; Phytochemicals

1. Introduction

In today's environment, antibiotic-resistant bacteria have grown to be a major concern. Numerous acute or chronic illnesses, including sepsis, inflammation, and ultimately cancer, can be carried on by these bacteria. Nowadays, searching for antimicrobial drugs is necessary because it is hard to find novel antibiotics that are effective against microbial pathogens. Through the appropriate use of antimicrobial drugs, disease-causing microorganisms have developed drug resistance [1, 2]. Different types of bacteria are developing resistance to these antimicrobial drugs that are already in the market, seriously endangering public health. There is a need for the development of innovative bactericides. Therefore, it is essential to develop efficient and affordable methods for the synthesis of therapeutic molecules to address the above mentioned health problems. The use of existing resources to create new solutions is made possible by nanotechnology [3]. Nanotechnology has endowed humanity with a plethora of nanoparticles that are widely used in industrial, biological, chemical, physicochemical, and other disciplines. Many metal oxide nanoparticles are "nano-antibiotics" because they can be used as antibacterial agents [4]. These metal oxide nanoparticles such as gold, silver [5], magnesium oxide, titanium dioxide, and zinc oxide along with carbon nanomaterials have distinctive physiochemical properties. Among these, gold nanoparticles (AuNPs) have received the most attention and have been widely used practically in various disciplines. By combining the unique properties of graphene with the advantages of metallic nanoparticles, a class of nanocomposite known as graphene and metal nanoparticle hybrid structures can exhibit unique physical properties. Because of their special characteristics, AuNPs decorated graphene oxides are attractive materials for usage in a variety of applications [6]. GrNs is a single layer of sp^2-hybridized carbon atoms

organized in a honeycomb-shaped two-dimensional (2-D) crystal lattice. It has high surface area, good antibacterial properties [7], high conductivity, and can be made easily and cheaply on a large scale [8]. Due to the widespread use of GrNs, environmental effects are a subject of considerable concern. Environmental and health problems are considerably increasing by using extremely toxic and dangerous substances, such as dimethyl hydrazine, hydroquinone, hydrazine hydrate, and hydrazine [9]. Thus, the search for an alternative method or a non-toxic reductant has increased recently. In order to avoid use of toxic and dangerous materials, many researchers have worked to find the environment friendly green methods for synthesizing graphene [10]. AuNPs have attracted the attention among existing nanomaterials because gold is an inert, oxidation-resistant substance, making its use fascinating in nanoscale technologies and devices [11, 12]. Moreover, AuNPs are good drug transporters that can enhance the antibacterial properties of loaded antibacterial medicines [13]. Functionalized AuNPs can be an effective medium for photothermal treatments to kill bacteria since they have photothermal properties. Many materials can acquire crucial antibacterial characteristics by including functional AuNPs [12, 14]. In recent years, many nanomaterials have been formed by using plants' wastes and their parts, bacteria, and fungi [15]. Plants are better options for producing nanomaterials since they are typically harmless, offer organic capping agents, and reduce the cost of toxic reducing chemicals [16, 17]. In the present research article, analysis of phytoconstituents and antioxidant properties of *P. edulis* and *S. cumini* leaves extracts was studied. Then the synthesis of AuNPs was done by utilizing an environment friendly process by reducing $HAuCl_4.3H_2O$ using phytochemicals (from *P. edulis* leaf extract) for the first time, which served as both reducing and capping agent. Greater dispersion of AuNPs on the surface of GrNs synthesized by employing *S. cumini* leaf extract, was achieved. Comparative antibacterial study of the biosynthesized AuNPs, GrNs and their nanocomposite (AuNPs-GrNs) was investigated against some pathogenic bacteria including, *B. subtilis* (Gram+), *S. aureus* (Gram+), *E. coli* (Gram-), and *P. aeruginosa* (Gram-).

2. Experimental section

2.1 Materials and chemicals

Tetrachloroauric (III) acid ($HAuCl_4.3H_2O$, orange crystals, purity $\leq$ 99.9% trace metal basis), and graphite (flakes, 99% carbon basis), all were purchased from Sigma Aldrich, sodium nitrate ($NaNO_3$), sulphuric acid (H_2SO_4), potassium permanganate ($KMnO_4$), hydrochloric acid (HCl), hydrogen peroxide (H_2O_2), ethanol, alumina slurry, silica gel, ammonium hydroxide (NH_4OH), ferric chloride ($FeCl_3$), lead acetate, chloroform, sodium hydroxide (NaOH), Folin Ciocalteu's (FC) reagent, *Passiflora edulis* (Krishna phal) and *Syzygium cumini* (Black plum) leaves were collected from nearby places, nutrient broth medium (Himedia), Agar Agar type-1 (Titan Biotech Ltd), sodium chloride (NaCl 99.5%, LOBA CHEMIE PVT. LTD), Bacterial strains (Gram +ve: *B. subtilis*, *S. aureus*; Gram -ve: *E. coli*, *P. aeruginosa*). Double distilled water (DDW) was used during the whole experiment.

2.2 Apparatus

Fourier transform infrared spectroscopy (FTIR, Bruker), X-ray diffractometer (XRD, Smart Lab 3 kW, Rigaku), Transmission electron microscope (Tecnai, HR-TEM), Field-emission scanning electron microscope (FE-SEM), Energy-Dispersive X-ray spectroscopy (EDX), ZETA-sizer/potential (Malvern Nano ZS), UV-spectrophotometer (Shimadzu, UV 3600 PLUS), Rivotek ultrasonic cleaner, vortex-shaker (SPINIX), centrifuge refrigerator, and laboratory water-bath (REMI), Bunsen Burner, laminar-air flow cabinet, L-shaped sterile spreader.

2.3 Plants extract preparation

2.3.1 *Passiflora edulis* leaves extract

P. edulis leaves were collected and cleaned with running tap water three or four times, followed by washing with double-distilled water. After cleaning, these *P. edulis* leaves were allowed to air dry for a couple of days (at room temperature). 15 g of these crushed leaves were boiled in 100 mL double-distilled water. The extract was filtered in doublet by using whatman filter (having a pore size of 2.5 µM) paper to achieve a fine solution (named as sample 1).

2.3.2 *Syzygium cumini* leaves extract

S. cumini leaves were collected and cleaned by using running tap water and deionized water. After being air dried at room temperature, leaves were gently ground in a motor pestle. 2.5 g of the dried leaves powder were mixed in 100 mL of deionized water and heated for 60 minutes at 50 °C. The leaf extract was then filtered in doublet by using whatmann filter paper to achieve a very fine solution (named as sample 2).

2.4 Analysis of phytoconstituents of plant extracts

Presence of phytochemicals in *P. edulis* and *S. cumini* leaf extracts were observed by following conventional method. The following protocols were used to perform a preliminary phytochemical screening of several secondary metabolites in the leaf extracts of *P. edulis* and *S. cumini*. The presence of alkaloids, phenols, steroids, flavonoids, saponins, tannins, anthraquinones, and cardiac glycoside were qualitatively screened in the extracted samples [18–20].

2.4.1 Quinone and anthraquinone detection (NH_3OH test)

1 mL of plant extracts were mixed separately with one drop of concentrated NH_3OH.

2.4.2 Phenols determination test

2.4.2.1 Ferric chloride test

Two drops of $FeCl_3$ solution were added to 1 mL of each solvent extract.

2.4.3 Tannins analysis

Two drops of 1% lead acetate were mixed with 0.5 mL of each solvent extracts.

2.4.4 Test for saponins

10 mL of distilled water and 0.5 mL of each solvent extract were mixed separately and then forcefully agitated in a graduated cylinder for 15 minutes.

2.4.5 Glycosides analysis

2.4.5.1 Salkowski's test

1 mL of each solvent extracts were combined with 0.5 mL of chloroform separately. Then carefully filled with 0.5 mL of concentrated H_2SO_4 and shaken gently.

2.4.6 Testing of flavonoids (NaOH test)

2.4.6.1 Alkaline test

In each solvent extract (0.5 mL) two drops of NaOH solution was added. When diluted with HCl the change in the color was observed.

2.4.6.2 Steroids test

In 6 mL of chloroform, 0.5 mL of each solvent extract was dissolved separately and an equal volume of concentrated H_2SO_4 was added.

2.5 Determination of total phenolic contents (TPC)

TPC was calculated by using Folin Ciocalteu's (FC) reagent method [19]. After adding the plant extracts (samples 1 and 2) into distilled water, 0.15 mL of FC reagent was added. Then 500 µL of sodium carbonate solution (20% w/v) was added and well mixed with a vortex shaker after 5 minutes of incubation. After 30 minutes of dark incubation, the tubes were checked for absorbance at 595 nm. Using gallic acid as a reference, the results were represented as gallic acid equivalents (GAE) [21].

2.6 In Vitro antioxidant assay

2.6.1 DPPH Assay

Plant leaf extracts were tested for their ability to scavenge DPPH free radicals by following Szollosi et al., with some modifications [19, 22]. The extracts of different concentrations (20, 40, 60, 80, 100, and 200 in µL) were taken in various test tubes. Various methanol concentrations (2980, 2960, 2940, 2920, 2900, and 2800 in µL) and freshly prepared DPPH solution (1 mL, 0.006%, w/v) were added in various test tubes. After being vortexed, the reaction mixture and the reference standards (ascorbic acid and butylated hydroxytolune) were left at room temperature in the dark for 30 minutes. The final step was to measure the absorbance at 517 nm of the solutions. Methanol was used as a blank and 1 mL of DPPH mixed with 2 mL of methanol was used as a control (Table 1). The following equation was used to determine the capacity to scavenge the DPPH radical:

$$\text{DPPH scavenged } (\%) = \frac{A_c - A_s}{A_c} \times 100 \qquad (1)$$

Where,
A_C - Absorbance of control
A_S - Absorbance in the presence of extract sample

2.6.2 Phosphomolybdate Method

Phosphomolybdate was used to test the antioxidant ability of plant extracts (samples 1 and 2) under an acidic pH by Brand William et al., with some modifications [23]. Plant extracts (0.1 mL) were mixed with the phosphomolybdate reagent (28 mM sodium phosphate, 4 mM ammonium molybdate, and 0.6 mM sulfuric acid) and incubated for 30 minutes at 95 °C. Then samples were cooled down and their absorbance was measured at 517 nm at room temperature. The readings were obtained against a reference of gallic acid solution in methanol and the control solution was a methanolic phosphomolybdate reagent.

2.7 Green synthesis of gold nanoparticles (AuNPs)

In order to form AuNPs in a sustainable manner, 150 mL of double-distilled water was taken in a 250 mL beaker flask. 10 mM Tetrachloroauric (III) acid was added in boiled 150 mL of double-distilled water while being stirred continuously. A lemon-yellow hue was observed that confirmed the development of gold salt solution after 10 minutes of stirring. For the reduction process, *P. edulis* leaf extract (10 mL) was slowly added to 140 mL of the prepared gold solution. As AuNPs formed, the solution's color progressively shifted from lemon yellow to dark purple [24].

2.8 Green synthesis of Graphene nanosheets (GrNs)

2.8.1 Synthesis of graphene oxide (GO)

Here, improved Hummer's method was used to form GO. Initially, a 500 mL reaction flask containing 1 g of graphite powder, 1.5 g of sodium nitrate ($NaNO_3$), 8 mL of double distilled water and 16.32 mL of H_2SO_4 (98%) were mixed and agitated for 30 minutes in an ice water bath. After finishing the ice water bath agitation, 4 g of potassium permanganate was gently added over the course of 10 to 15 minutes and the mixture was stirred at 40 °C for 90 minutes. After that, 50 mL of double-distilled water was gradually

Table 1. Preparation of plant's leaf extracts for DPPH scavenging.

Test tubes	DPPH (mL)	Methanol (µL)	Plants extract (µL)
Blank	-	2000	-
Control	1	2000	-
I	1	2980	20
II	1	2960	40
III	1	2940	60
IV	1	2920	80
V	1	2900	100
VI	1	2800	200

added over the course of 15 minutes, and the mixture was then stirred at 70 °-80 °C for an additional hour. Following the addition of 100 mL of lukewarm (40 °C) distillate water, a brown suspension was produced [25]. 12 mL of 30% H_2O_2 solution was used to treat this dark suspension. To get rid of extra manganese, the graphene oxide dispersion was rinsed with 5% HCl and then with deionized water until neutrality was attained. Then dried at 60 °C in an oven for about 3 hours or until fine and moisture less powder of GO was achieved.

2.8.2 Biosynthesis of GrNs

In order to form GrNs, produced GO was reduced by using this finely prepared solution of *S. cumini* plant leaves extract. A 250 mL beaker flask containing 30 mL of deionized water was loaded with 30 mg of GO (1 mg/mL) and the mixture was agitated for 60 minutes. After adding 25 mL of leaf extract and stirring the mixture for five hours at 60 °C, it was homogeneous. The homogeneous mixture was maintained on a magnetic stirrer for a further 48 hours at room temperature followed by sonication for 90 minutes. The homogeneous mixture was then cleaned with deionized water and dried in an oven for five hours [25, 26].

2.9 Characterization of AuNPs and GrNs

TEM, FTIR, UV-Spectroscopy and Zeta-sizer/potential were used to confirm the formation of AuNPs and GrNs. Shift in colour quickly (yellow to purple) confirmed the bio-reduction of Au^+ to Au^0.

2.10 Formation of AuNPs-GrNs nanocomposite by single-step method

To form the nanocomposite (AuNPs-GrNs), 10 mL of the GrNs solution (3.5 mg/mL) was sonicated for up to 30 minutes followed by continuous stirring at 40 °C for an additional 90 minutes. This aqueous GrNs solution was then mixed with 10 mL of green synthesized AuNPs solution and the mixture was agitated for an additional 24 hours at room temperature. After preparation, any impurities and undispersed AuNPs were removed from the AuNPs-GrNs nanocomposite's solution by centrifuging and cleaning them with ethanol and water. The nanocomposite was then dried in a lab oven at 60 °C to produce the fine powder [26, 27].

2.10.1 Characterization of AuNPs-GrNs nanocomposite

The morphology, size, stability, dispersity, and elemental composition of the nanocomposite were studied by employing UV-visible spectra and Zeta-sizer/Potential-Nano-ZS (Aryabhata CIL, M.D.U., Rohtak, Hr. India), FE-SEM, EDX and HR-TEM (AIIMS, New Delhi, India), FTIR (CIL, Chandigarh), X-ray Diffraction (HAU, Hisar, Hr. India).

2.11 Application of fabricated AuNPs, GrNs and AuNPs-GrNs nanocomposite in analyzing antimicrobial effectiveness

2.11.1 Preparation of bacterial culture

Gram-positive (*B. subtilis, S. aureus*) and gram-negative (*E. coli, P. aeruginosa*) bacteria were revived. In order to revive the bacteria, broth was made. For that 3.1 g of nutrient broth (NB) was added to 125 mL of DW. Four test tubes were filled with freshly made nutrient agar (15 mL). These test tubes were tightly closed and kept for incubation at 37 °C for 24 hours [28].

2.11.2 Preparation of agar-plates

To prepare the agar plates, 5 g nutrient broth (NB) and 4 g agar were mixed in 200 mL DW. This media was kept in autoclave at 121 °C for 20 minutes. Then the media was taken in petri-plates and left them for solidifying. Media is actually the substance which provides nutrients for the growth of the microorganisms [29].

2.11.3 Agar-well diffusion assay (AWDA)

The antibacterial effects of AuNPs, GrNs and AuNPs-GrNs nanocomposites were evaluated using AWDA against gram-positive (*B. subtilis, S. aureus*) and gram-negative (*E. coli, P. aeruginosa*) [30, 31]. AWDA is a popular method for assessing the antimicrobial activity. A volume of the microbial inoculum (100 µL) was dispersed across the whole surface of the agar plate to inoculate it. After using a sterile cork borer to aseptically punch a hole with a diameter of 8 mm, the antimicrobial agents (AuNPs, GrNs and AuNPs-GrNs) were added to the well in the desired concentration. Different concentrations of the AuNPs, GrNs and AuNPs-GrNs (25 µg/mL, 50 µg/mL, 100 µg/mL, and 200 µg/mL) were poured into the wells of agar plates [7]. After that, these agar plates were incubated for 24 hours at 37 °C. These antimicrobial agents spread across the agar media and prevented the bacterial strains from growing. By following the incubation period, the growth inhibition zones' diameters in mm were assessed.

2.11.4 Determination of Minimum inhibitory concentration (MIC)

The smallest drug concentration that suppresses the apparent microorganism growth is known as the minimum inhibitory concentration (MIC). Drugs with lower MIC value are more effective antimicrobial agents because they suppress the growth of the microorganism with little dose of the drug. To determine the MIC value, bacteria were cultured on plates with solid growth medium [18].

3. Results and discussion

3.1 Analysis of phytochemicals of *P. edulis* and *S. cumini* leaves extract

The findings indicated that *P. edulis* leaf extract contained anthraquinones, phenols, saponins, and alkalines and *S. cumuni* extract comprised of anthraquinones, phenols, glycosides, alkalines and steroids (Table 2). Anthraquinone's residency was shown by the emergence of a red color after two minutes of mixing of plant extract with NH_3OH. The development of a bluish-black hue indicates the presence of phenols. The presence of tannins was confirmed by appearance of yellow precipitate when leaf extracts were mixed with the lead acetate. The formation of foams showed the presence of saponins. The presence of glycosides was indicated by a reddish-brown color. When diluted with HCl the strong yellow color that had formed turned colorless, indicating the presence of flavonoids. The sulphuric acid

Table 2. Qualitative phytochemistry of *S. cumini* and *P. edulis* leaf extracts.

No.	Phytochemicals	Plants extracts	
		Passiflora edulis	*Syzygium cumini*
1.	Anthraquinone	+	+
2.	Phenols	+	+
3.	Tannins	-	-
4.	Saponins	+	-
5.	Glycosides	-	+
6.	Alkaline	+	+
7.	Steroids	-	+

(+) Present, (-) Absent.

layer became yellow with green fluorescence as the upper layer turned red. This suggests that steroids were present in the leaf extracts. The phytochemical screening test actually aids in isolating and characterizing the chemical constituents present in the plant extracts. These secondary plant metabolites stimulated the reducing ability, which assisted in reducing the precursor (Tetrachloroauric (III) acid and graphene oxide).

3.2 Analysis of total phenolic contents (TPC) of plant's extracts

In air-dried leaves, the content of polyphenols, which was responsible for reduction and capping of AuNPs and GrNs was quantified for *P.edulis* and *S. cumuni* to be 296.56 ± 72.18 mgGAE/g and 266.56 ± 35.27 mgGAE/g respectively (Table 3).

3.3 Analysis of antioxidant capacity of plant's extracts

3.3.1 Scavenging of DPPH

Lower down of extent of the violet staining of DPPH radical's was a sign of the antioxidant's capacity to scavenge free radicals. The assay was followed according to Szollosi et al., 2002 (Fig. 1) [22].

3.3.2 Phosphomolybdate assay (PMA)

The reduction of Mo (VI) to Mo (V) by the plant extract containing antioxidant chemicals is the fundamental idea behind the phosphomolybdenum assay which is used to

Table 3. Total TPC and TAC of plant extracts of sample 1 (*P.edulis* leaf extract) and sample 2 (*S. cumuni* leaf extract).

Samples	Total phenolic content (mg GAE/g)	Total Antioxidant capacity (mg GAE/g)
Sample 1	296.566 ± 72.188	9.647 ± 0.281
Sample 2	266.566 ± 35.276	8.209 ± 0.191

Values are expressed as mean $\pm$ SD ($n = 3$). The absorbance against the reagent blank was determined at 595 nm and 517 nm with a UV-Visible spectrometer for phenolics and antioxidant capacity respectively. Both were expressed as mg gallic acid equivalents (GAE).

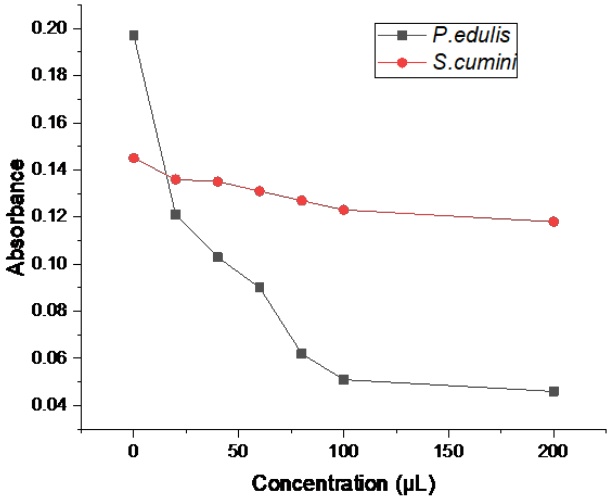

Figure 1. Antioxidative property of leaves extract of *P. edulis* and *S. cumini* during DPPH scavenging.

evaluate antioxidant capability. Green color mixtures were formed. The number of antioxidants in the solution was determined by the intensity of the green colour. Leaf extracts of *P.edulis* and *S. cumuni* were found to have a significant overall antioxidant capacity of 9.647 ± 0.281 and 8.209 ± 0.191 respectively because of the presence of phenolic compounds [32, 33] (Table 3).

3.4 Characterization of green synthesized AuNPs

The hue of the solution changed from yellow lemon color to a purple tint as gold nanoparticles formed. It is significant to note that since phytochemicals already functioned as reducing and capping agents there was no need to add external stabilizing agents.

3.4.1 UV-visible spectroscopy

A UV-visible spectrum was used to confirm the formation of AuNPs. The results showed that the *P. edulis* leaf extract showed a peak at around 460 nm (Fig. 2a.i), whereas the tetrachloroaurate solution did not show a clear peak (Fig. 2a.ii). However, Fig. 2a.iii shows that a broad peak appeared at 575 nm when *P. edulis* leaf extract was added to a tetrachloroaurate solution. Further analysis has demonstrated that this peak represented the formation of spherically shaped, monodisperse AuNPs [34–36].

3.4.2 Fourier transform infrared (FTIR) spectroscopy

For the purpose of identifying different functional groups present in *P. edulis* leaf extract, FTIR analysis of green synthesized AuNPs was conducted. The FTIR spectra of AuNPs are shown in Fig. 2b. A long peak seen at 3401.82 cm^{-1} was attributed to O-H bonds, indicating the existence of phenolic compounds. The polypeptides from *P. edulis* acted as capping agents for the AuNPs, previously reported by Nguyen et al. [37]. The band at 2921.66 cm^{-1} represented the aldehydic (C-H) bond. In addition the band at 1,647.83 cm^{-1} can be attributed to the vibrational modes of C=C double bonds. The small stretching peaks were also seen around 1265.70 cm^{-1}, which was close to the frequency of C=O stretching. In a study, it was proven via infrared spectroscopy that the carbonyl group creates amino acids and proteins which aid in capping and stabilizing the metal nanoparticles and minimizes their agglomeration. Thus, the FTIR analysis suggests that proteins might be responsible for stabilizing and capping the AuNPs [24, 38, 39].

3.4.3 Zeta-potential/Sizer

Zeta potential (ZP) value provided details about the stability and surface charge of synthesized AuNPs. The extract that was used to synthesize AuNPs, had a zeta potential measurement of -7.80 mV (Fig. 2c) and polydispersive index (PDI) value of 0.694 (Fig. 2d). Because of this, the reading of AuNPs showed acceptable stability and at least the required steady expression [40]. The distinctive peaks in the zeta-sizer (Fig. 2d) revealed that the AuNPs had an average diameter in the range of 28.77 nm [41, 42].

3.4.4 Transmission electron microscope (TEM)

The TEM was used to analyze the formed AuNPs' size and shape, as shown in Fig. 2e. The AuNPs' spherical shape and good separation from one another were analyzed by using TEM. The fact that the *P. edulis* leaf extract matrix was evenly distributed around the AuNPs suggests that it worked as a capping agent to prevent the AuNPs from aggregating. The formed AuNPs had an average size of 100 nm.

3.5 Characterization of GrNs

Particularly in the field of nanotechnology, GrNs have been one of the most fascinating areas of study in recent years. Graphene has recently attracted scientists' interest due to its unique properties. Pure natural graphite was chemically oxidized to yield GO, which was subsequently reduced by using *S. cumuni* and exfoliated to produce GrNs.

3.5.1 UV-visible spectroscopy

The UV-visible absorption spectrum for GrNs was displayed in Fig. 3a. Electronic absorption spectra of the particles between 200-300 nm in a water solvent were recorded at room temperature using a UV-visible spectrometer. The UV-visible absorption peak of GrNs was achieved at 260 nm [43, 44].

3.5.2 Fourier transform infrared spectroscopy

The peaks in Fig. 4b with centres at 3288.67 cm^{-1} can be explained by the stretching and bending modes of the OH-group, which showed the presence of physisorbed water linked with the products. The peaks at 1647.04 cm^{-1} and 1039.77 cm^{-1} corresponded to C=C conjugation and C-C band stretching vibrations respectively, are used to illustrate the FTIR spectra of GrNs [43, 45].

3.5.3 Zeta-potential/Sizer

Zeta potential is an important signal for determining the surface charge of the sheets and for defining the stability of the dispersion. GrNs was supposed to form a stable suspension at zeta potentials of -26.0 mV due to interparticle electrostatic attraction (Fig. 3b). GrNs had a diameter of 838.7 nm and a PDI value of 0.494, as seen in Fig. 3c.

3.5.4 Transmission electron microscope

The findings show that GrNs are made up of a few thin layers which are layered on top of one another with little folding or creasing. TEM analysis revealed that synthesized GrNs has a 2D-nanosheet like structure in nano-range (i.e. 200 nm) Fig. 3d.

3.6 Characterization of AuNPs-GrNs nanocomposite

3.6.1 UV-visible spectroscopy

The appearance of absorbance bands at 280 nm and 520 nm (green line), which are typical of GrNs and AuNPs surface plasmon resonance bands respectively, suggests the creation of AuNPs on the graphene sheets after the formation of AuNPs-GrNs hybrid nanomaterials (Fig. 4a) [44, 46, 47].

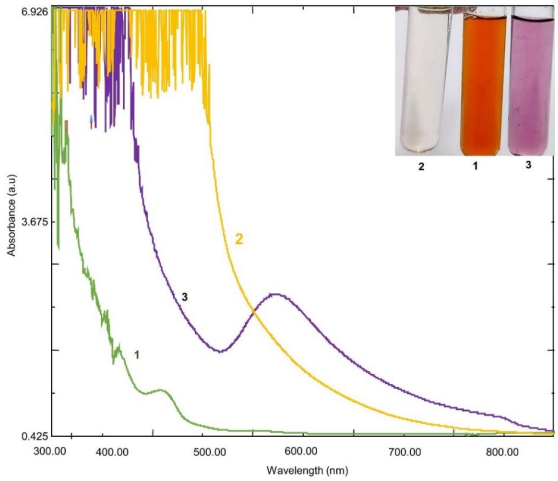

(a)

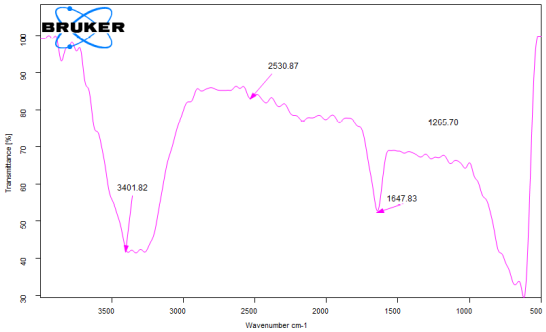

(b)

		Mean (mV)	Area (%)	St Dev (mV)
Zeta Potential (mV): -7.80	Peak 1:	-7.80	100.0	3.45
Zeta Deviation (mV): 3.45	Peak 2:	0.00	0.0	0.00
Conductivity (mS/cm): 1.48	Peak 3:	0.00	0.0	0.00
Result quality Good				

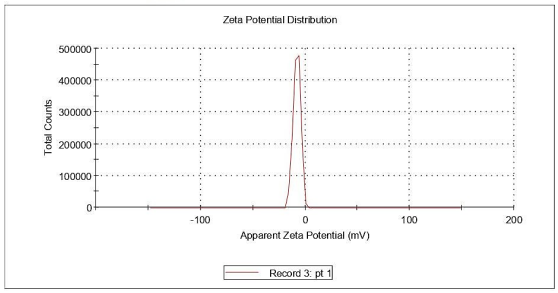

(c)

		Size (d.n...	% Intensity:	St Dev (d.n...
Z-Average (d.nm): 28.77	Peak 1:	55.43	81.8	29.11
PdI: 0.694	Peak 2:	3.969	14.2	1.440
Intercept: 0.841	Peak 3:	4923	4.0	661.6

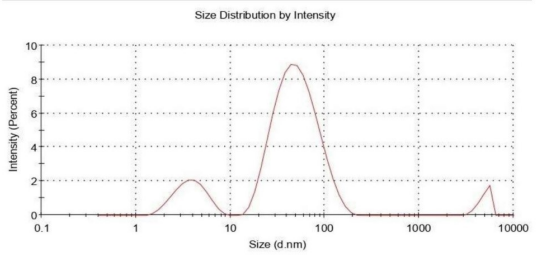

(d)

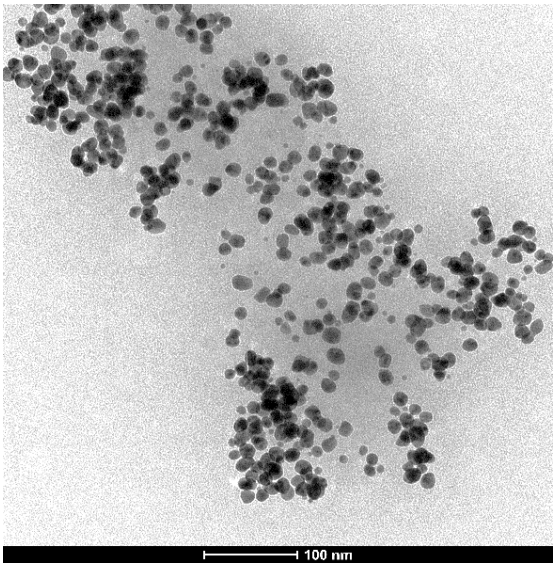

(e)

Figure 2. Characterization of green synthesized AuNPS by (a) UV-visible spectroscopy showing absorbance at 575 nm (b) FTIR-spectra (c) Zeta-potential (d) Zeta-sizer/PDI (e) Transmission electron microscope showing 100 nm size.

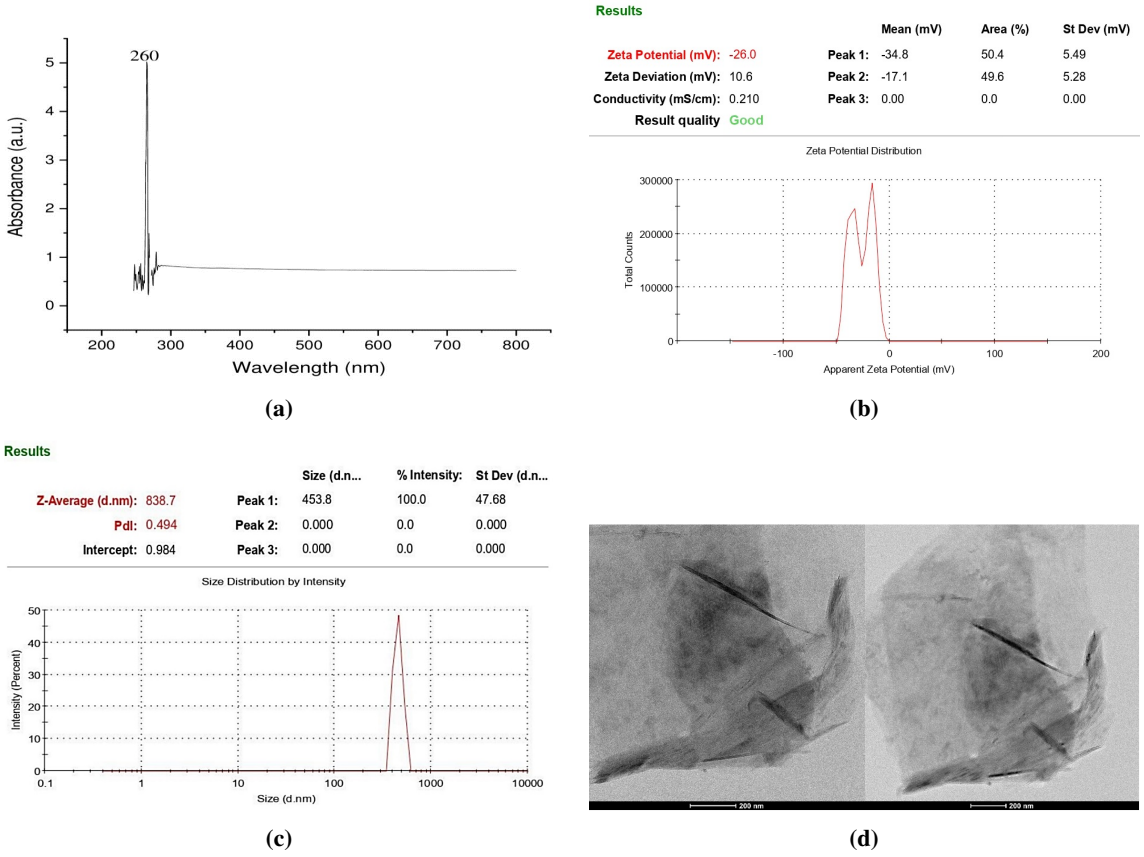

Figure 3. Characterization of GrNs (a) UV-visible spectroscopy (b) FTIR-spectroscopy (b) Zeta-potential (c) Zeta-sizer/PDI (d) TEM showing 200 nm size.

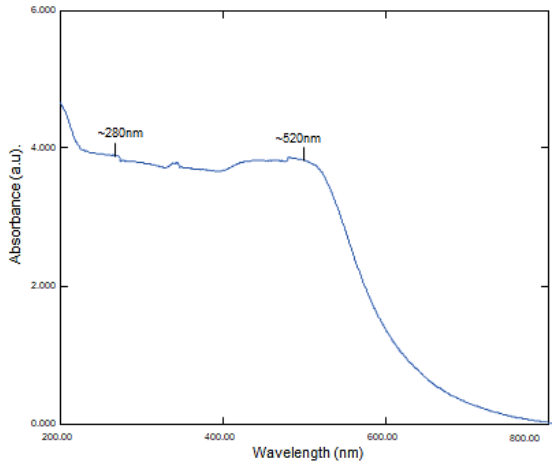

(a)

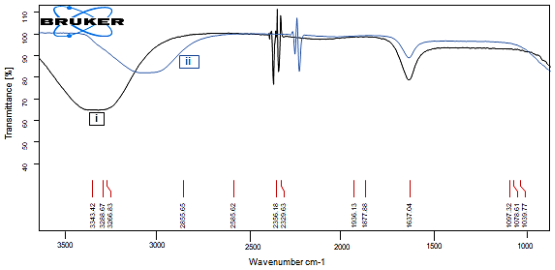

(b)

	Mean (mV)	Area (%)	St Dev (mV)
Zeta Potential (mV): -31.1	Peak 1: -31.1	100.0	5.46
Zeta Deviation (mV): 5.46	Peak 2: 0.00	0.0	0.00
Conductivity (mS/cm): 0.0615	Peak 3: 0.00	0.0	0.00
Result quality Good			

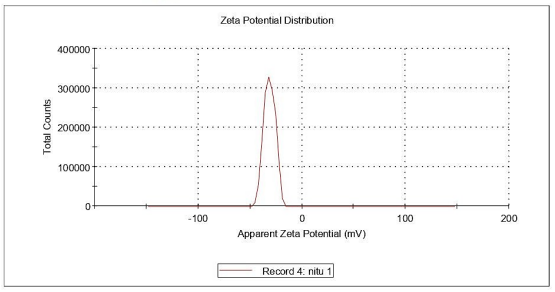

(c)

Results

		Size (d.n...	% Intensity:	St Dev (d.n...
Z-Average (d.nm): 1780	Peak 1:	1432	100.0	306.5
PdI: 0.321	Peak 2:	0.000	0.0	0.000
Intercept: 0.928	Peak 3:	0.000	0.0	0.000

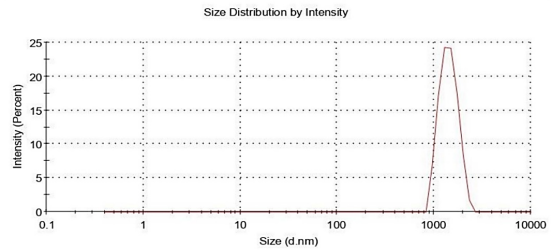

(d)

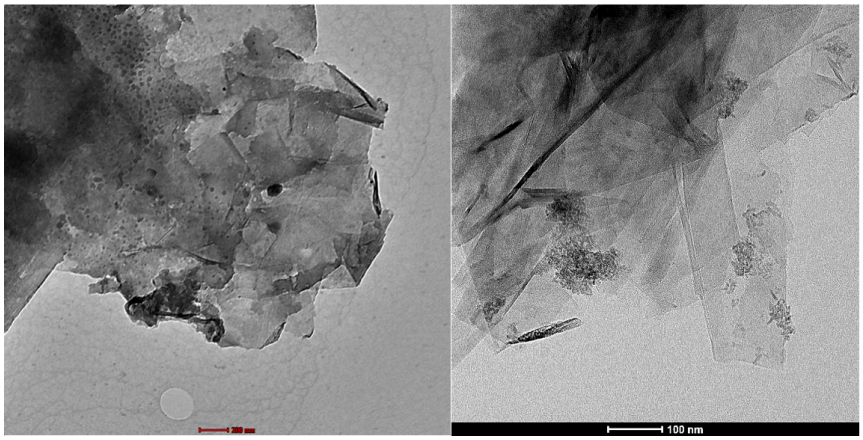

(e)

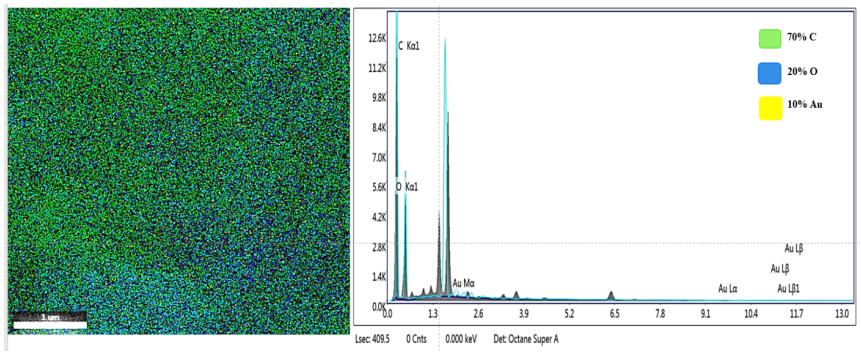

(f)

Figure 4. Characterization of AuNPs-GrNs by (a) UV-visible spectroscopy (b) Zeta-potential (c) Zeta-sizer/PDI (d) TEM (e) FTIR-spectra of i. GrNs, ii. AuNPs-GrNs (f) EDAX of AuNPs-GrNs showing the elemental composition (C, O, and Au).

3.6.2 FTIR spectroscopy

It was shown that in AuNPs-GrNs nanocomposite, the intensity of the entire band dropped. By combining with GrNs to form an AuNPs-GrNs nanocomposite, AuNPs nanoparticles caused the wavenumber to shift from 3288.67 cm^{-1} to 3185.00 cm^{-1} and 1637.04 cm^{-1} to 1625.92 cm^{-1} (Fig. 4b) [48, 49].

3.6.3 Zeta-potential/Sizer

Zeta potential was used to measure the surface charge of the AuNPs-GrNs nanocomposite. Due to electrostatic repulsion, nanocomposites with zeta potential of -31.1 mV were regarded as stable (Fig. 4c). The average diameter and PDI value of AuNPs-GrNs nanocomposite were 1780 nm and 0.321 respectively showing in Fig. 4d measured by zeta-sizer.

3.6.4 Transmission electron microscope

The TEM images (Fig. 4e) demonstrated that the AuNPs were well dispersed across the whole GrNs and were spherical in shape. Additionally, it was demonstrated that the majority of the particles were on the GrNs, demonstrating that these AuNPs also aids in the stabilization of GrNs.
The success preparations of GrNs, AuNP, and the uniform distribution of the AuNPs on the GrNs to create the AuNPs-GrNs nanocomposite (Fig. 4f) are all clearly shown by these data.

3.7 Antibacterial activity analysis

3.7.1 Determination of Minimum inhibitory concentration (MIC)

The MIC values of AuNPs, GrNs, and AuNPs- GrNs nanocomposite were determined by using the well diffusion method by utilizing cultures of *S. aureus* (Gram+), *B. subtilis* (Gram+), *E. coli* (Gram-), and *P. aeruginosa* (Gram-). One of the most useful methods for assessing antibacterial activity is the zone of inhibition (ZI) [50, 51]. It was discovered that the antibacterial activities of the AuNPs, GrNs, and AuNPs-GrNs nanocomposite against the bacterial pathogens were dose-dependent. AuNPs (Fig. 5a), GrNs (Fig. 5b), and AuNPs-GrNs (Fig. 5c) at doses ranging from 25 to 200 µg/mL were treated. AuNPs-GrNs nanocomposite showed a synergistic effect. By using nanocomposite rather than AuNPs and GrNs individually, clear zones of inhibition for all bacterial species were achieved (Table 4).

3.7.2 Comparative analysis of AuNPs, GrNs and AuNPs-GrNs nanocomposite in bactericidal effect

The zones of inhibition (ZI) approach was used to compare the bactericidal effect of AuNPs, GrNs, and AuNPs-GrNs on various bacterial strains (*S. aureus*- 96, *B. subtilis*- 121, *E. coli*- 243, and *P. aeruginosa*- 424). The ZI for *S. aureus* was 5 mm (AuNPs), 10 mm (GrNs), 15 mm (AuNPs-GrNs); *B. subtilis* 5 mm (AuNPs), 9 mm (GrNs), 10 mm (AuNPs-GrNs); *E. coli* 0 mm (AuNPs), 12 mm (GrNs), 25 mm (AuNPs-GrNs); and *P. aeruginosa* 5 mm (AuNPs), 10 mm (GrNs), 10 mm (AuNPs-GrNs) (Table 5). AuNPs-GrNs nanocomposite demonstrated the highest ZI among all the treated materials. It is clear that combining graphene-based materials with AuNPs had an impact on how antibacterial they were, leading to a synergistic bactericidal effect. The observations are shown in Fig. 6.

4. Conclusion

Phytochemical analysis and antioxidant properties of leaf extracts of *P. edulis* and *S. cumini* were observed. Antibiotics, insect growth inhibitors, repellents, antifungal, antibacterial, antiviral, and other medical properties are all fought off by phytochemical compounds. These phytoconstituents serve as reducing agents for reducing nanoparticles. Phytoconstituents present in *P. edulis* are anthraquinone, phenols, saponins, and alkalines while in *S. cumini*; anthraquinone, phenols, glycosides, alkalines and steroids are present. Total TPC present in *P. edulis* and *S. cumini* was 296.566 ± 72.188 and 266.566 ± 35.276 mg GAE/g respectively and TAC present in *P. edulis* and *S. cumini* was 9.647 ± 0.281 and 8.209 ± 0.191 mg GAE/g respectively. These leaf extracts were then employed

Table 4. Shows the MIC value of AuNPs, GrNs, and AuNPs-GrNs on gram-positive (*S. aureus* and *B. subtilis*) and gram-negative (*E. coli* and *P. aeruginosa*) bacterial species.

S. No.	Bacterial species	Labeled petri plates	AuNPs MIC (µg/mL)	GrNs MIC (µg/mL)	AuNPs-GrNs MIC (µg/mL)
1.	*S.aureus* (Gram+)	96	100	100	50
2.	*B. subtilis*(Gram+)	121	50	100	25
3.	*E.coli* (Gram-)	243	200	200	25
4.	*P. aeruginosa* (Gram-)	424	100	200	25

Table 5. Comparative Zones of inhibition (ZI) of bactericidal effects of AuNPs, GrNs, and AuNPs-GrNs nanocomposites.

S. No.	Bacterial species	Labelled on Petri plates	AuNPs ZI (mm)	GrNs ZI (mm)	AuNPs-GrNs ZI (mm)
1.	*S.aureus* (Gram+)	96	5	10	15
2.	*B. subtilis* (Gram+)	121	5	9	10
3.	*E.coli* (Gram-)	243	0	12	25
4.	*P. aeruginosa* (Gram-)	424	5	10	11

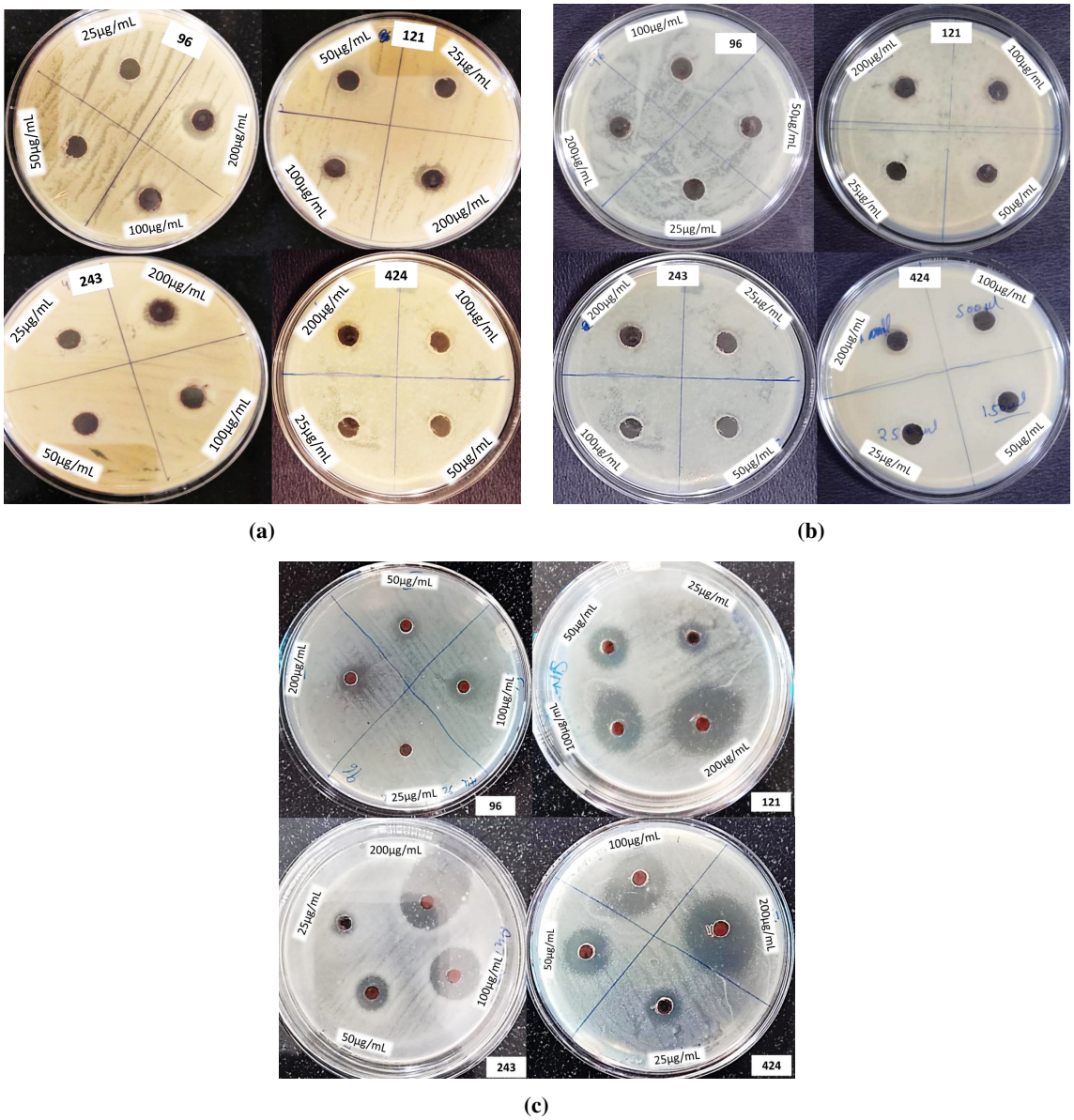

Figure 5. Minimum inhibitory concentration (MIC) value of (a) GrNs (b) AuNPs, and (c) AuNPs-GrNs nanocomposites against gram-positive (96-*S. aureus*, 121-*B. subtilis*) and gram-negative bacteria (243-*E. coli* and 424-*P. aeruginosa*).

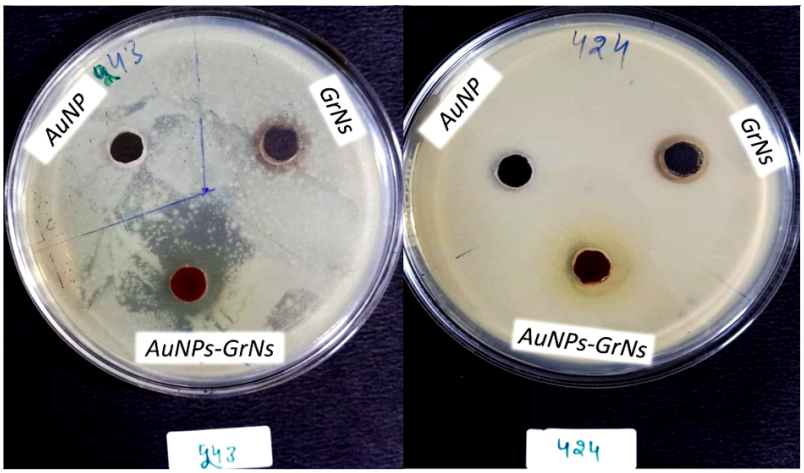

Figure 6. Antibacterial activity of AuNPs, GrNs, and AuNPs-GrNs against gram-positive (96-*Staphylococcus aureus*, 121-*B. subtilis*) and gram-negative bacteria (243- *E. coli* and 424-*P. aeruginosa*).

for the green synthesis of AuNPs and GrNs to lower the use of toxic chemicals. The elemental composition, stability, dispersity, size and shape of nanoparticles and their nanocomposites were characterized by UV-visible spectra and Zeta-sizer/Potential-Nano-ZS, FE-SEM, EDX, HR-TEM, FTIR, and X-ray Diffraction. A comparative bactericidal effect of these green synthesized AuNPs, GrNs and their AuNPs-GrNs nanocomposites was studied. A range of dose concentrations of AuNPs, GrNs, and AuNPs-GrNs from 25-200 µg/mL were used. The MIC values of nanomaterials and their nanocomposites were determined. MIC values of AuNPs (*S. aureus* 100 µg/mL; *B. subtilis* 50 µg/mL; *E. coli* 200 µg/mL; *P. aeruginosa* 100 µg/mL), GrNs (*S. aureus* 100 µg/mL, *B. subtilis* 100 µg/mL; *E.coli* 200 µg/mL; *P. aeruginosa* 200 µg/mL) and AuNPs-GrNs (*S. aureus* 50 µg/mL, *B. subtilis* 25 µg/mL; *E.coli* 25 µg/mL; *P. aeruginosa* 25 µg/mL) were analyzed. The inhibitory efficiency was shown to be high at high dosage concentrations (i.e. 200 µg/mL) for *S. aureus* 10 mm (AuNPs), 14 mm (GrNs), and 15 mm (AuNPs-GrNs); *B. subtilis* 8 mm (AuNPs), 12 mm (GrNs), 35 mm (AuNPs-GrNs); *E. coli* 7 mm (AuNPs), 11 mm (GrNs), 35 mm (AuNPs-GrNs); and for *P. aeruginosa* 10 mm (AuNPs), 8 mm (GrNs), and 38 mm (AuNPs-GrNs). The comparative bactericidal effect of AuNPs, GrNs and AuNPs-GrNs nanocomposite was observed by treating these various bacterial strains, i.e., AuNPS (*S. aureus* 5 mm; *B. subtilis* 5 mm; *E.coli* 0 mm; *P. aeruginosa* 5 mm), GrNs (*S. aureus* 10 mm; *B. subtilis* 9 mm; *E.coli* 12 mm; *P. aeruginosa* 10 mm), and for AuNPs-GrNs (*S. aureus* 15 mm; *B. subtilis* 10 mm; *E.coli* 25 mm; *P. aeruginosa* 10 mm) mentioned in the study. Comparatively, the bactericidal impact of the AuNPs-GrNs nanocomposite was more efficient than that of AuNPs and GrNs against the bacterial isolates. AuNPs-GrNs nanocomposite, which has been biosynthesized, is economical and eco-friendly. As confirmed by the Zeta-potential analyzer, AuNPs-GrNs nanocomposites possessed good stability and gave synergistic bactericidal effect compared to AuNPs and GrNs individually. AuNPs-GrNs a green biocomposite was recognized in this regard for its promising potential for usage in biomedical and food industry applications.

Acknowledgments
Sarita Yadav, one of the authors, expresses gratitude for the technical assistance provided by SAIF-AIIMS New-Delhi, India, ACIL M.D. University, Hr. India, and CIL-PU Chandigarh, India.

Authors Contributions
Sarita Yadav: Conceptualization, Investigation, Analysis, Methodology, Writing - Review & Editing, Data curation, Validation.
Neetu Sehrawat: Artwork, Evaluation, Plagiarism, Bibliography.
Minakshi Sharma: Supervision.

Availability of Data and Materials
The data that support the findings of this study are available from the corresponding author upon reasonable request.

Conflict of Interests
The authors declare that they have no known competing financial interests or personal relationships that could have appeared to influence the work reported in this paper.

Funding
The authors declare that no funds, grants, or other support were received during the work.

Ethical Approval
Authors of the research confirm that the research did not involve participation of any human or animal subjects.

References

[1] S. Maiti, D. Krishnan, G. Barman, S.K. Ghosh, and J.K Laha. "Antimicrobial activities of silver nanoparticles synthesized from Lycopersicon esculentum extract. ". *Journal of Analytical Science and Technology*, **5**(1):1–7, 2014. DOI: https://doi.org/10.1186/s40543-014-0040-3.

[2] Y. Feng, Q. Chen, Q. Yin, G. Pan, Z. Tu, and L Liu. "Reduced graphene oxide functionalized with gold nanostar nanocomposites for synergistically killing bacteria through intrinsic antimicrobial activity and photothermal ablation.". *ACS Applied Bio Materials*, **2**(2):747–756, 2019. DOI: https://doi.org/10.1021/acsabm.8b00608.

[3] M. Adil, T. Khan, M. Aasim, A.A. Khan, and M Ashraf. "Evaluation of the antibacterial potential of silver nanoparticles synthesized through the

interaction of antibiotic and aqueous callus extract of Fagonia indica.". *AMB Express*, **9**(1), 2019. DOI: https://doi.org/10.1186/s13568-019-0797-2.

[4] A.K. Bhardwaj, V. Kumar, V. Pandey, R. Naraian, and R. Gopal. "Bacterial killing efficacy of synthesized rod shaped cuprous oxide nanoparticles using laser ablation technique.". *SN Applied Sciences*, **1**:1–8, 2019.

[5] A.K. Bhardwaj, A. Shukla, S. Maurya, S.C. Singh, K.N. Uttam, S. Sundaram, and R. Gopal. "Direct sunlight enabled photo-biochemical synthesis of silver nanoparticles and their Bactericidal Efficacy: Photon energy as key for size and distribution control.". *Journal of Photochemistry and Photobiology B: Biology*, **188**:42–49, 2018. DOI: https://doi.org/10.1016/B978-0-444-52204-7.X5017-2.

[6] A.M. Díez-Pascual. "Antibacterial action of nanoparticle loaded nanocomposites based on graphene and its derivatives: A mini-review.". *International Journal of Molecular Sciences*, **21**(10), 2020. DOI: https://doi.org/10.3390/ijms21103563.

[7] N. Thiyagarajulu, S. Arumugam, A.L. Narayanan, T. Mathivanan, and R.R. Renuka. "Green synthesis of reduced graphene nanosheets using leaf extract of tridax procumbens and its potential in vitro biological activities.". *Biointerface Research in Applied Chemistry*, **11**(3):9975–9984, 2020. DOI: https://doi.org/10.33263/BRIAC113.99759984.

[8] B. Campbell and J. Manning. "The rise of victimhood culture: Microaggressions, safe spaces, and the new culture wars.". *The Rise of Victimhood Culture: Microaggressions, Safe Spaces, and the New Culture Wars*, :1–265, 2018. DOI: https://doi.org/10.1007/978-3-319-70329-9.

[9] Z. Khosroshahi, M. Kharaziha, F. Karimzadeh, and A. Allafchian. "Green reduction of graphene oxide by ascorbic acid.". *AIP Conference Proceedings*, **1920**, 2018. DOI: https://doi.org/10.1063/1.5018941.

[10] M. Gaur, C. Misra, A.K. Bajpayee, and A.K. Bhardwaj. "Recent advances in agriculture waste for nanomaterial production.". *Green and Sustainable Approaches Using Wastes for the Production of Multifunctional Nanomaterials*, :331–344, 2024.

[11] S. Balasubramanian, S.M.J. Kala, and T.L. Pushparaj. "Biogenic synthesis of gold nanoparticles using Jasminum auriculatum leaf extract and their catalytic, antimicrobial, and anticancer activities.". *Journal of Drug Delivery Science and Technology*, **57**:101620, 2020. DOI: https://doi.org/10.1016/j.jddst.2020.101620.

[12] C. Su, K. Huang, H.H. Li, Y.G. Lu, and D.L. Zheng. "Antibacterial properties of functionalized gold nanoparticles and their application in oral biology.". *Journal of Nanomaterials*, **2020**, 2020. DOI: https://doi.org/10.1155/2020/5616379.

[13] S. Veena, T. Devasena, S.S.M. Sathak, M. Yasasve, and L.A. Vishal. "Green synthesis of gold nanoparticles from vitex negundo leaf extract: Characterization and in vitro evaluation of antioxidant–antibacterial activity.". *Journal of Cluster Science*, **30**(6):1591–1597, 2019. DOI: https://doi.org/10.1007/s10876-019-01601-z.

[14] S. Priya Velammal, T.A. Devi, and T.P. Amaladhas. "Antioxidant, antimicrobial and cytotoxic activities of silver and gold nanoparticles synthesized using Plumbago zeylanica bark.". *Journal of Nanostructure in Chemistry*, **6**(3):247–260, 2016. DOI: https://doi.org/10.1007/s40097-016-0198-x.

[15] A.S. Bharti, C. Baran, A.K. Bhardwaj, S. Tripathi, R. Pandey, and K.N. Uttam. "Domestic waste utilization in the synthesis of functional nanomaterial.". *Green and Sustainable Approaches Using Wastes for the Production of Multifunctional Nanomaterials, Elsevier*, :61–76, 2024.

[16] S.K. Panda, Y.K. Mohanta, L. Padhi, Y.H. Park, T.K. Mohanta, and H. Bae. "Large scale screening of ethnomedicinal plants for identification of potential antibacterial compounds.". *Molecules*, **21**(3):1–20, 2016. DOI: https://doi.org/10.3390/molecules21030293.

[17] A.K. Bhardwaj, R. Naraian, S. Sundaram, and R. Kaur. "Biogenic and non-biogenic waste for the synthesis of nanoparticles and their applications.". *Bioremediation: Green Approaches for a Clean and Sustainable Environment, CRC Press*, :207–218, 2022. DOI: https://doi.org/10.1364/OE.18.012311.

[18] K. Alemayehu. "Phytochemical analysis, antibacterial and antioxidant activity of the leave extracts of ruta chalepensis.". *Chemistry and Materials Research*, **11**(6):1–7, 2019. DOI: https://doi.org/10.7176/cmr/11-6-01.

[19] T. Kumari and V. Shukla. "Validation of phytochemicals, antioxidant activity and characterization of green synthesized iron nanoparticles: A comparison.". *Journal of Applied and Natural Science*, **13**(3):1102–1110, 2021. DOI: https://doi.org/10.31018/jans.v13i3.2894.

[20] S.D. Ramaiya, J.S. Bujang, and M.H. Zakaria. "Assessment of total phenolic, antioxidant, and antibacterial activities of passiflora species.". *The Scientific World Journal*, **2014**, 2014. DOI: https://doi.org/10.1155/2014/167309.

[21] S. Jan, M.R. Khan, U. Rashid, and J. Bokhari. "Assessment of antioxidant potential, total phenolics and flavonoids of different solvent fractions of monotheca buxifolia fruit.". *Osong Public Health and Research Perspectives*, **4**(5):246–254, 2013. DOI: https://doi.org/10.1016/j.phrp.2013.09.003.

[22] R. Szollosi and I. Szollosi Varga. "Total antioxidant power in some species of Labiatae (Adaptation of FRAP method).". *Acta Biologica Szegediensis*, **46**(3-4):125–127, 2002.

[23] W. Brand-Williams, M.E. Cuvelier, and C. Berset. "Use of a free radical method to evaluate antioxidant activity.". *LWT - Food Science and Technology*, **28** (1):25–30, 1995. DOI: https://doi.org/10.1016/S0023-6438(95)80008-5.

[24] T. My-Thao Nguyen, T. Anh-Thu Nguyen, N. Tuong-Van Pham, Q.V. Ly, T. Thuy-Quynh Tran, T.D. Thach, C.L. Nguyen, K.S. Banh, V.D. Le, L.P. Nguyen, D.T. Nguyen, C.H. Dang, and T.D. Nguyen. "Biosynthesis of metallic nanoparticles from waste Passiflora edulis peels for their antibacterial effect and catalytic activity.". *Arabian Journal of Chemistry*, **14**(4):103096, 2021. DOI: https://doi.org/10.1016/j.arabjc.2021.103096.

[25] N.K. Kadiyala, B.K. Mandal, S. Ranjan, and N. Dasgupta. "Bioinspired gold nanoparticles decorated reduced graphene oxide nanocomposite using Syzygium cumini seed extract: Evaluation of its biological applications.". *Materials Science and Engineering C*, **93**(June):191–205, 2018. DOI: https://doi.org/10.1016/j.msec.2018.07.075.

[26] S. Yadav and M. Sharma. "Construction of a cytochrome c nanosensor based on nano-engineered cytochrome oxidase enzyme covalently immobilized on AuNPs-GrNs nanocomposite-modified pencil graphite electrode.". *Journal of Materials Science*, **58**(40):15780–15804, 2023. DOI: https://doi.org/10.1007/s10853-023-09006-0.

[27] A. Marinoiu, M. Raceanu, M. Andrulevicius, A. Tamuleviciene, T. Tamulevicius, S. Nica, D. Bala, and M. Varlam. "Low-cost preparation method of well dispersed gold nanoparticles on reduced graphene oxide and electrocatalytic stability in PEM fuel cell.". *Arabian Journal of Chemistry*, **13**(1):3585–3600, 2020. DOI: https://doi.org/10.1016/j.arabjc.2018.12.009.

[28] A.K. Bhardwaj, A. Shukla, R.K. Mishra, S.C. Singh, V. Mishra, K.N. Uttam, and R. Gopal. "Power and time dependent microwave assisted fabrication of silver nanoparticles decorated cotton (SNDC) fibers for bacterial decontamination.". *Frontiers in Microbiology*, **8**:330, 2017.

[29] A.K. Bhardwaj and R. Naraian. "Cyanobacteria as biochemical energy source for the synthesis of inorganic nanoparticles, mechanism and potential applications: a review.". *3 Biotech*, **11**(10):445, 2021.

[30] N. Rabiee, S. Ahmadi, O. Akhavan, and R. Luque. "Silver and gold nanoparticles for antimicrobial purposes against multi-drug resistance bacteria.". *Materials (Basel, Switzerland)*, **15**(5):1799, 2022. DOI: https://doi.org/10.3390/ma15051799.

[31] S. Sathiyaraj, G. Suriyakala, A.D. Gandhi, R. Babujanarthanam, K.S. Almaary, T.W. Chen, and K. Kaviyarasu. "Biosynthesis, characterization, and antibacterial activity of gold nanoparticles.". *Journal of Infection and Public Health*, **14**(12):1842–1847, 2021.

[32] P. Prieto, M. Pineda, and M. Aguilar. "Spectrophotometric quantitation of antioxidant capacity through the formation of a ... .". *Analytical Biochemistry*, **269**:337–341, 1999. DOI: https://doi.org/10.1037/a0037168.

[33] A. Ali, H. Wu, E.N. Ponnampalam, J.J. Cottrell, F.R. Dunshea, and H.A.R. Suleria. "Comprehensive profiling of most widely used spices for their phenolic compounds through lc-esi-qtof-ms2 and their antioxidant potential.". *Antioxidants*, **10**(5), 2021. DOI: https://doi.org/10.3390/antiox10050721.

[34] E.E. Abel, P.R. John Poonga, and S.G. Panicker. "Characterization and in vitro studies on anticancer, antioxidant activity against colon cancer cell line of gold nanoparticles capped with Cassia tora SM leaf extract.". *Applied Nanoscience (Switzerland)*, **6**(1): 121–129, 2016. DOI: https://doi.org/10.1007/s13204-015-0422-x.

[35] J.K. Suthar, R. Rokade, A. Pratinidi, R. Kambadkar, and S. Ravindran. "Purification of nanoparticles by liquid chromatography for biomedical and engineering applications.". *American Journal of Analytical Chemistry*, **08**(10):617–624, 2017. DOI: https://doi.org/10.4236/ajac.2017.810044.

[36] N. Barnawi, S. Allehyani, and R. Seoudi. "Biosynthesis and characterization of gold nanoparticles and its application in eliminating nickel from water.". *journal of materials research and technology*, **17**:537–545, 2022. DOI: https://doi.org/10.1016/j.jmrt.2021.12.013.

[37] H.H. Nguyen, J. Park, S. Kang, and M. Kim. "Surface plasmon resonance: A versatile technique for biosensor applications.". *Sensors (Switzerland)*, **15**(5):10481–10510, 2015. DOI: https://doi.org/10.3390/s150510481.

[38] S. Srivastava and A. Pandey. "Syngonium podophyllum leaf extract mediated synthesis and characterization of gold nanoparticles for biosensing potential: A sustainable approach.". *Current Nanoscience*, **17**(1):81–89, 2015. DOI: https://doi.org/10.2174/1573413716999200507125437.

[39] B. Sadeghi, M. Mohammadzadeh, and B. Babakhani. "Green synthesis of gold nanoparticles using Stevia rebaudiana leaf extracts: Characterization and their stability.". *Journal of Photochemistry and Photobiology B: Biology*, **148**:101–106, 2015. DOI: https://doi.org/10.1016/j.jphotobiol.2015.03.025.

[40] K. Xin Lee, K. Shameli, M. Miyake, N. Kuwano, N.B. Bt Ahmad Khairudin, S.E. Bt Mohamad, and Y.P. Yew. "Green synthesis of gold nanoparticles using aqueous extract of garcinia mangostana fruit peels.". *Journal of Nanomaterials*, **2016**, 2016. DOI: https://doi.org/10.1155/2016/8489094.

[41] N. Abdel-Raouf, N.M. Al-Enazi, and I.B.M. Ibraheem. "Green biosynthesis of gold nanoparticles using Galaxaura elongata and characterization of their antibacterial activity.". *Arabian Journal of Chemistry*, **10**:S3029–S3039, 2017. DOI: https://doi.org/10.1016/j.arabjc.2013.11.044.

[42] M.V. Sujitha and S. Kannan. "Green synthesis of gold nanoparticles using Citrus fruits (Citrus limon, Citrus reticulata and Citrus sinensis) aqueous extract and its characterization.". *Spectrochimica Acta - Part A: Molecular and Biomolecular Spectroscopy*, **102**:15–23, 2013. DOI: https://doi.org/10.1016/j.saa.2012.09.042.

[43] T.F. Emiru and D.W. Ayele. "Controlled synthesis, characterization and reduction of graphene oxide: A convenient method for large scale production.". *Egyptian Journal of Basic and Applied Sciences*, **4**(1):74–79, 2017. DOI: https://doi.org/10.1016/j.ejbas.2016.11.002.

[44] B. Vellaichamy, P. Prakash, and J. Thomas. "Synthesis of AuNPs@RGO nanosheets for sustainable catalysis toward nitrophenols reduction.". *Ultrasonics Sonochemistry*, **48**(January):362–369, 2018. DOI: https://doi.org/10.1016/j.ultsonch.2018.05.012.

[45] S. Joshi, R. Siddiqui, P. Sharma, R. Kumar, G. Verma, and A. Saini. "Green synthesis of peptide functionalized reduced graphene oxide (rGO) nano bioconjugate with enhanced antibacterial activity.". *Scientific Reports*, **10**(1):1–11, 2020. DOI: https://doi.org/10.1038/s41598-020-66230-3.

[46] Z. Osváth, A. Deák, K. Kertész, G. Molnár, G. Vértesy, D. Zámbó, C. Hwang, and L.P. Biró. "The structure and properties of graphene on gold nanoparticles.". *Nanoscale*, **7**(12):5503–5509, 2015. DOI: https://doi.org/10.1039/c5nr00268k.

[47] N.A. Ali and F.M. Yasin. "Synthesis and characterization of silver and gold nanoparticles decorated reduced graphene oxide.". *AIP Conference Proceedings*, **2151**(August), 2019. DOI: https://doi.org/10.1063/1.5124647.

[48] F. Yousefimehr, S. Jafarirad, R. Salehi, and M.S. Zakerhamidi. "Facile fabricating of rGO and Au/rGO nanocomposites using Brassica oleracea var. gongylodes biomass for non-invasive approach in cancer therapy.". *Scientific Reports*, **11**(1):1–13, 2021. DOI: https://doi.org/10.1038/s41598-021-91352-7.

[49] B. Sadeghi, M.A.S. Sadjadi, and A. Pourahmad. "Effects of protective agents (PVA & PVP) on the formation of silver nanoparticles.". *International Journal of Nanoscience and Nanotechnology*, **4**(1):3–12, 2008.

[50] B. Sadeghi. "Synthesis of silver nanoparticles using leaves aqueous extract of Nasturtium Officinale (NO) and its antibacterial activity.". *International Journal of Molecular and Clinical Microbiology*, **4**(2):428–434, 2014.

[51] A.M. Díez-Pascual. "Antibacterial action of nanoparticle loaded nanocomposites based on graphene and its derivatives: A mini-review.". *International Journal of Molecular Sciences*, **21**(10):3563, 2020.